Modulating phonon transport in bilayer black phosphorus: Unraveling the interplay of strain and interlayer quasicovalent bonds

Rongkun Chen [1], Shiqian Hu [2,*], Weina Ren [1,†], and Chunhua Zeng [1,‡]

[1]*Faculty of Science, Kunming University of Science and Technology, Kunming 650500, People's Republic of China*
[2]*School of Physics and Astronomy, Yunnan University, Kunming 650091, People's Republic of China*

Efficient thermal management in nanoscale electronic devices presents a pressing challenge. The two-dimensional (2D) materials, notably bilayer black phosphorus, exhibit unique thermal properties that hold promise for addressing this challenge. In this study, we explore the impact of the strain on phonon hydrodynamics in bilayer black phosphorus, providing insight into its intricate thermal behavior. By employing first-principles calculations and the Boltzmann transport equation, we uncover that the thermal conductivity generally decreases with increasing strain. However, a nonmonotonic behavior emerges at small strains, challenging conventional expectations. This behavior is attributed to the intricate interplay among the softening of optical phonons induced by strain, the subsequent enhancement of phonon scattering, and the maintenance/strengthening of the quadratic Z-axis acoustic (ZA) mode through reinforced quasicovalent bonds, ultimately contributing to improved phonon hydrodynamics. Our findings underscore the pivotal role of interlayer thickness in governing these effects. Our research pioneers the modulation of phonon hydrodynamics, offering transformative insight into the 2D materials' thermal behavior.

I. INTRODUCTION

As electronic devices continue to shrink towards the nanoscale, their power density per unit area has surged, presenting formidable challenges in thermal management and energy conversion at this reduced length scale [1–3]. Researchers have responded to these challenges by focusing on two-dimensional (2D) materials, drawn to their unique thermal properties. Understanding the phonon transport in 2D materials is a critical aspect of their design and implementation. Recent studies have uncovered numerous factors influencing the heat transport properties in solids, including coherent phonons, phonon-phonon interactions, boundary scattering, defects and impurities, symmetry-breaking phenomena, and phonon renormalization [4–9]. Among these factors, strain modulation stands out, capturing significant research attention due to its reversible advantages.

One noteworthy application of strain modulation is found in black phosphorus [10–16], an exceptional 2D material known for its distinctive nonplanar folding structure. In its single-layer form, black phosphorus exhibits intriguing properties such as a negative Poisson's ratio and weak resonance bonds between atoms, resulting in remarkably low thermal conductivity [17–19]. However, when the black phosphorus forms a bilayer, the interlayer interactions change, marked by the strong quasicovalent bonds alongside the van der Waals forces [20–25]. Recent research in black phosphorus has re-vealed that the in-plane strain applied to multilayer black phosphorus can uniquely modify the quasicovalent bond coupling between layers [23–25]. This strain sensitivity enables precise manipulation of the band gap size and the induction of semiconductor-metal transitions, highlighting the potential of the strain in 2D materials [10–12,26–29].

Conversely, phonon hydrodynamics, a kinetic behavior of the phonon transport similar to the fluid transport, has become an active area of research due to its potential for enhancing the thermal conductivity of materials [30–39]. The phenomenon can be induced in 2D materials like graphene, diamondlike bilayer graphene, hexagonal boron nitride, and transition metal dichalcogenides, with normal-type scattering dominating even at room temperature and beyond [40–43]. This is achieved through the manipulation of their dimensionality, structure, and composition [9,29,33,44]. These studies pave the way for a deeper understanding of heat flow in 2D materials. Moreover, the examination of thermal conductivity evolution in thin graphite underscores a correlation between high thermal conductivity, thickness, and phonon hydrodynamics, thereby spotlighting the unique thermal properties of graphene and its counterparts [45].

The study of phonon hydrodynamics provides a tangible framework for understanding heat transport in dielectric solids and semiconductors [46]. It offers practical insight into high thermal conductivity materials, particularly in graphitic materials [47], and identifies graphite as a three-dimensional material supporting phonon hydrodynamics at higher temperatures [48]. Poiseuille phonon flow phenomena in thin graphite reveal size-dependent thermal conductivity [49], while suspended graphene exhibits distinct temperature and sample width-dependent thermal conductivity behaviors [50].

*Corresponding author: shiqian@ynu.edu.cn
†wnren@kust.edu.cn
‡chzeng83@kust.edu.cn

Exploration of second sound phenomena in graphite and high-frequency second sound in bulk natural Ge expands understanding of phonon hydrodynamics [51–53], offering different avenues for exploring thermal management and energy conversion technologies. However, despite the growing interest in phonon hydrodynamics, most of the current research has focused on discovering its physical mechanisms, with little research done on modulating or controlling phonon hydrodynamics.

Recent research in the field of the bilayer *AB*-stacked graphene has revealed that when subjected to out-of-plane compressive strain, the interlayer van der Waals forces (vdW) between graphene layers significantly strengthen [54]. This strengthening induces a gradual weakening of phonon hydrodynamic transport, as indicated by the observed change in the ratio of $\kappa_{iterative}/\kappa_{RTA}$. Here, $\kappa_{iterative}$ and κ_{RTA} represent the material thermal conductivity calculated using iterative solution and relaxation time approximation (RTA) methods, respectively. The RTA method erroneously assumes all phonon scattering processes as *U*-type scatterings, leading to an underestimation of thermal conductivity in materials exhibiting phonon hydrodynamic transport [35,55–58]. In contrast, the iterative solution accurately accounts for *N*-type scatterings, providing a reliable calculation of material thermal conductivity. Therefore, the ratio of thermal conductivities obtained by the two different methods, i.e., $\kappa_{iterative}/\kappa_{RTA}$, serves as a reliable indicator to determine the occurrence of phonon hydrodynamic transport in materials. Building upon the insight that interlayer interactions profoundly impact phonon hydrodynamic transport, and recognizing that in-plane strain can modify the quasicovalent bond coupling between layers in black phosphorus, we are driven to investigate the influence of in-plane strain and the coupling changes induced by in-plane strain on the quasicovalent bonds in bilayer black phosphorus on phonon hydrodynamics.

In our current research, we delve into the impact of the strain on the phonon hydrodynamics phenomenon and its modulation effects, particularly in the context of bilayer black phosphorus materials. Utilizing first-principles calculations and the Boltzmann transport equation (BTE), we investigate how thermal conductivity in black phosphorus material responds to strain applied along the zigzag direction. Our findings reveal that, within the 0–16% strain range, the thermal conductivity of black phosphorus generally decreases with the increasing strain. However, when the strain remains small (<4%), the relationship between the thermal conductivity and the strain exhibits a nonmonotonic behavior, initially decreasing and then increasing. To shed light on this nonmonotonic behavior, we analyze the phonon scattering rates and distinguish between *N*-type and *U*-type scattering. Our research unveils that this nonmonotonic behavior is a result of the strain's nonmonotonic modulation on *N*-type scattering, further affirming the strain's influence on the phonon hydrodynamics phenomenon. Furthermore, we elucidate that the changes in phonon hydrodynamics stem from alterations in the interlayer interactions due to the in-plane strain. This research holds great significance as it demonstrates the potential of the strain in modulating phonon hydrodynamics. It introduces fresh perspectives and provides theoretical support for advancing phonon transport modulation, offering valuable insight for the development and application of phononics.

II. COMPUTATIONAL METHODOLOGY

This study employs the Vienna *ab initio* Simulation Package (VASP) [59] for all first-principles computations, utilizing the projected augmented wave method within the framework of density functional theory (DFT). Our calculations are based on the Perdew-Burke-Ernzerhof (PBE) functional as the exchange-correlation function within the generalized gradient approximation (GGA) [60]. To account for the interlayer vdW interactions, we incorporate the optB88b exchange-correlation functional [61] in our analysis. This choice ensures accurate identification of charges and forces within and between the layers [17]. The convergence of results is achieved by optimizing the Hellmann-Feynman force and energy within the unit cell, employing a cutoff energy of 500 eV, until they reached convergence thresholds of 10^{-8} eV and 10^{-3} eV Å^{-1}, respectively. Furthermore, we adjust the Brillouin zone sampling k-mesh [62] grid to $16 \times 12 \times 1$ for the BP. For the extraction of second-order interaction force constants (IFCs) and third-order IFCs, we utilize the PHONOPY code [63] in conjunction with the thirdorder_vasp.py function [64]. These computations involve the construction of supercells with dimensions $6 \times 4 \times 1$ and $4 \times 3 \times 1$. To account for periodic mirroring in the out-of-plane directions, we include a substantial 20 Å vacuum region to prevent the unwanted interactions. Last, in determining the cutoff distance, we consider the interactions up to the 20th nearest neighbors, and for the thermal conductivity calculations, we employ a *Q* grid of dimensions $31 \times 31 \times 1$ based on our comprehensive convergence analysis (see details in Supplemental Material Sec. I [65]).

By employing an iterative method to solve the BTE based on the three-phonon scattering framework, we can derive the lattice thermal conductivity tensor, denoted as $\kappa^{\alpha\beta}$, using the ShengBTE package [64]:

$$\kappa^{\alpha\beta} = \frac{1}{k_B T^2 \Omega} \sum_{\lambda} f_0(f_0 + 1)(\hbar\omega_\lambda)^2 v_\lambda^\alpha F_\lambda^\beta. \tag{1}$$

In this equation, the k_B, T, and Ω represent the Boltzmann constant, temperature, and the system volume, respectively. The summation is performed over each phonon mode λ, uniquely defined by both the wave vector and phonon branch. Here, the $\hbar$, ω, f_0, and v denote the reduced Planck constant, phonon frequency, equilibrium Bose-Einstein distribution, and phonon group velocity, respectively. The indices α and β correspond to the Cartesian coordinates. The term F_λ^β signifies the linear coefficient of the nonequilibrium phonon distribution function given by $F_\lambda^\beta = \tau_\lambda^0(v_\lambda^\beta + \Delta_\lambda^\beta)$, where τ_λ^0 is the phonon lifetime obtained using the single-mode relaxation time approximation (RTA). The term Δ_λ^β is obtained through a fully iterative solution of the BTE and serves as a correction term to account for the deviations in the phonon distribution from the RTA scheme. In practical calculations, we can initiate the process with the RTA solution and iteratively solve the BTE to obtain the F_λ^β.
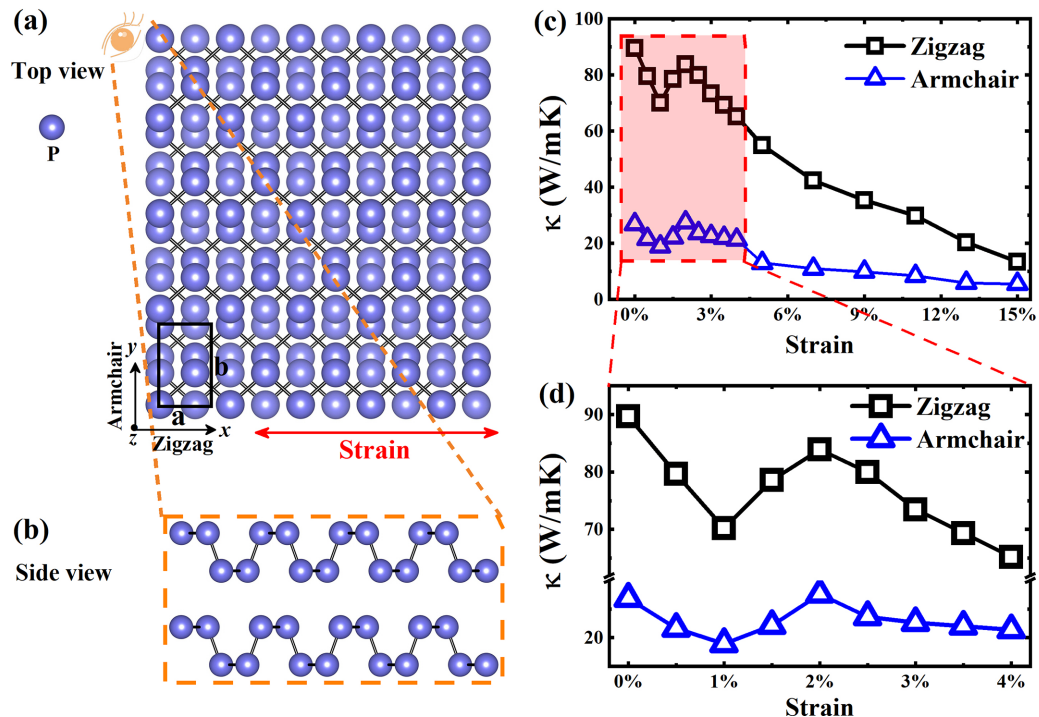
FIG. 1. Schematic representations of bilayer black phosphorus and its response to strain-induced changes in thermal conductivity. Panels (a) and (b) depict top and side views of bilayer black phosphorus structure. (c) The thermal conductivity at 300 K in the x and y directions under varying tensile strain conditions. (d) A magnified view of the small strain region ($<4\%$) from (c).

III. RESULTS AND DISCUSSION

Figures 1(a) and 1(b) depict the top and side views of bilayer black phosphorous. In the optimization process, the lattice constants are determined to be $a = 3.327$ Å and $b = 4.520$ Å. These values closely match those reported in previous works [66,67]. Figure 1(c) presents the results of thermal conductivity calculations of bilayer black phosphorous at 300 K. For unstrained bilayer black phosphorous, the thermal conductivities in the x and y directions are found to be 89.70 and 26.87 W/mK, respectively. These values are consistent with previous predictions [68,69].

Moreover, the thermal conductivity of bilayer black phosphorous typically exhibits a consistent trend of decline as the strain levels intensify, both in the x and y directions. In this context, the strain is defined as the percentage change in the lattice constant in the x direction, calculated as $(\Delta a / a) \times 100\%$, where Δa is the difference between the lattice constant before and after deformation, and a is the lattice constant before deformation. This trend in thermal conductivity can be elucidated by the strain-induced phonon softening, particularly for the optical phonon modes, showcased in Fig. 2(a), and leading to a gradual reduction in their group velocities, as illustrated in Fig. 2(b). Significantly, the most prominent consequence of this phonon softening is the gradual erosion of the material's band gap as strain increases. As strain intensifies, the band gap steadily diminishes until it eventually closes. Simultaneously, as the band gap shrinks, the material experiences a pronounced increase in the phonon scattering. This heightened scattering results from the greater availability of phonon states within the reduced band gap, leading to more frequent interactions and collisions between phonons. This

impact is vividly presented in the calculation of the three-phonon scattering phase space, as well as in the corresponding summation, depicted in Fig. 2(c) and its inset. Consequently, the phonon scattering rate, a metric measuring the frequency of phonon-phonon collisions, undergoes a significant increase [as illustrated in Fig. 2(d)]. This surge in phonon scattering profoundly influences the thermal transport properties of bilayer black phosphorous, ultimately contributing to the observed decrease in thermal conductivity under elevated strain levels.

However, within the small strain range ($<4\%$), the thermal conductivity of the bilayer black phosphorous exhibits a nonmonotonic behavior. It initially decreases before showing an increase, as clearly illustrated in Fig. 1(d) [a magnified view of the strain ranges 0–4% in Fig. 1(c)]. This unique behavior defies the conventional expectations based on the behavior of single-layer black phosphorus. In single-layer black phosphorus, the thermal conductivity typically experiences a monotonic decrease with increasing strain. This phenomenon is often attributed to changes in the fold structure, which refers to the alterations in the material's atomic arrangement due to the strain-induced deformation [70].

On the contrary, the nonmonotonic behavior observed in bilayer black phosphorus hints at a more complex interplay of factors. Previous experimental findings and theoretical calculations consistently emphasize the significance of interlayer quasicovalent bonds in 2D layered structures, particularly in bilayer black phosphorus [25]. These quasicovalent bonds, akin to quasibonds in covalent compounds, are shown by researchers to dominate interlayer interactions, resulting in distinct thermal and electronic properties. These properties
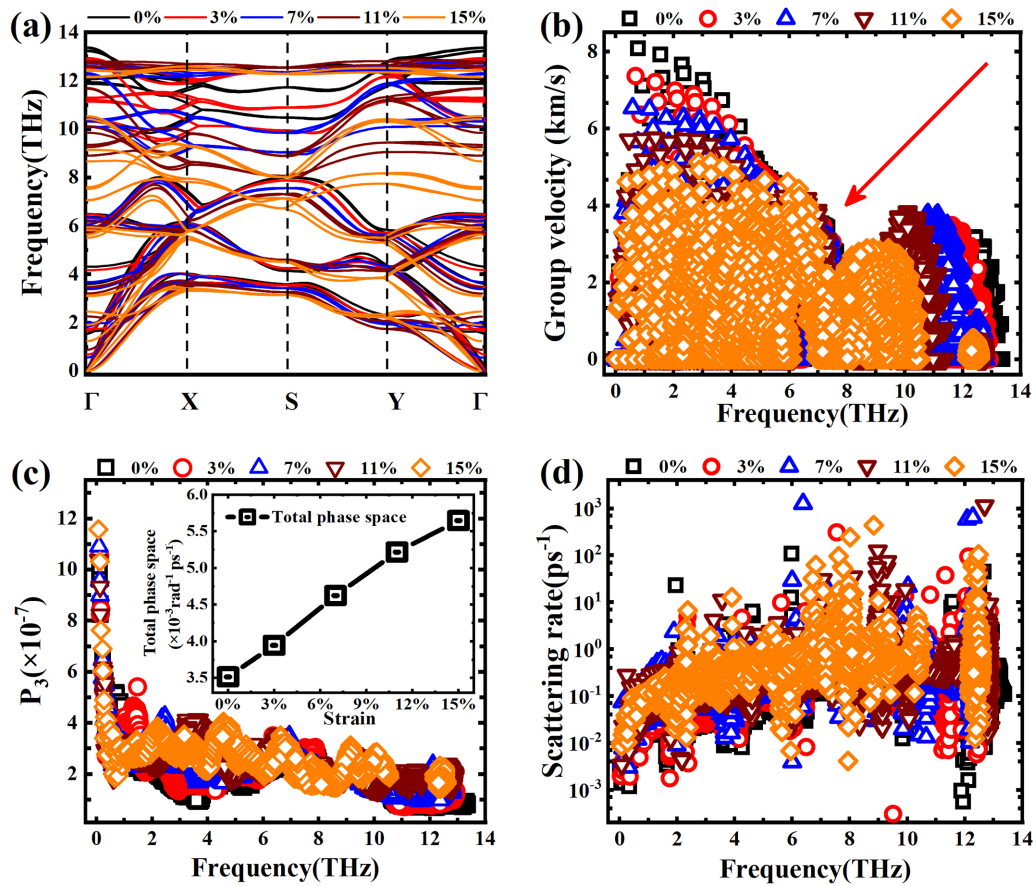
FIG. 2. The correlated phonon properties under the strain modulation. (a) The phonon dispersion, (b) the corresponding phonon group velocity, (c) the three-phonon scattering phase space with its corresponding summation in the inset, and (d) the scattering rates at various strain levels.

encompass a lower thermal conductivity and a substantial impact on the electronic structure [17,20–24].

In the case of bilayer black phosphorus, there are two thicknesses influencing interlayer coupling, primarily dominated by quasicovalent bonds, as depicted in the inset of Fig. 3(a): the intralayer thickness d and the interlayer thickness D. To gain further clarity on which thickness primarily governs the modulation of the thermal conductivity in response to the strain, we conduct calculations on the D and d variation under strain conditions. As illustrated in Fig. 3(a), under zero strain conditions, the intralayer distance d and interlayer distance D measure 2.144 and 3.196 Å,
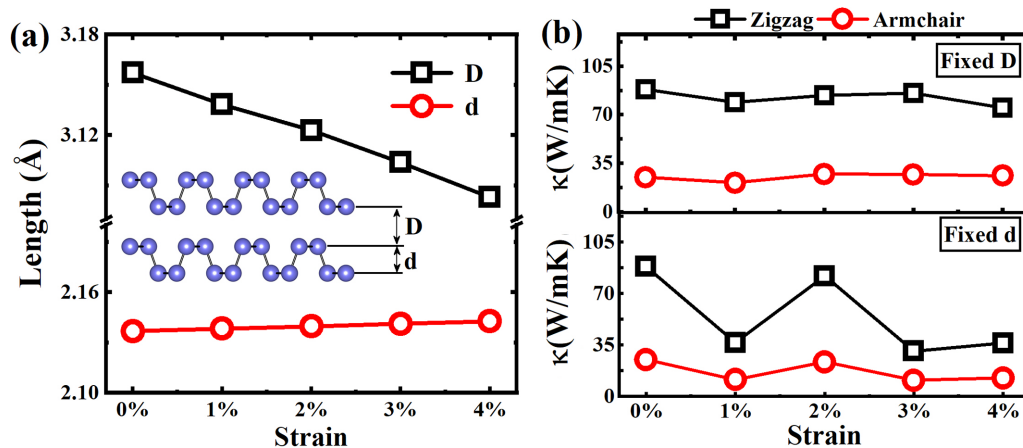

FIG. 3. Strain-induced changes in the thickness and the thermal conductivity. (a) Evolution of the intralayer thickness d and interlayer thickness D with varying strain. (b) The thermal conductivity variation under changing strain conditions with the interlayer thickness D or the intralayer distance d held constant.

respectively, which aligns consistently with prior studies [66]. Furthermore, our findings reveal a significant decrease in the interlayer thickness D, while intralayer thickness d exhibits only a minor increase. Notably, this shift in the intralayer thickness d is expected, given the previously documented negative Poisson's ratio phenomenon observed in single-layer black phosphorus within the prior study [18].

Collectively, these calculations strongly suggest that the shifts in the interlayer coupling primarily arise due to the variations in the interlayer thickness D induced by the applied strain. To further substantiate this conclusion, we conduct additional calculations where we artificially held either the interlayer thickness D or the intralayer distance d constant, observing the impact of the strain on thermal conductivity. Significantly, before conducting thermal conductivity calculations, our structure undergoes substantial relaxation when strain is applied at a fixed interlayer or intralayer spacing. Further details can be found in Supplemental Material Sec. II [65]. The research outcomes are depicted in Fig. 3(b). When the interlayer thickness D is kept constant, the thermal conductivity of bilayer black phosphorus remains nearly unchanged despite variations in the strain. However, when we fix the intralayer thickness d, the thermal conductivity exhibits a phenomenon akin to that seen in Fig. 1(d), characterized by a nonmonotonic behavior. This result provides further confirmation that the nonmonotonic phenomenon is indeed driven by changes in the interlayer coupling, specifically originating from variations in the interlayer thickness D.

Consequently, we speculate that the nonmonotonic behavior may originate from the interplay of various factors as the strain is applied. Notably, changes in the fold structure are accompanied by variations in the interlayer coupling due to the in-plane strain. These modifications influence the interaction between the two phosphorus layers within the bilayer structure, thereby affecting phonon transport differently compared to single-layer black phosphorus. The thermal conductivity initially decreases due to strain-induced phonon softening, leading to the enhanced phonon scattering. However, at a specific threshold, the altered interlayer coupling, underpinned by quasicovalent bonds, may start to dominate, resulting in an increase in thermal conductivity. This intricate interplay between the fold structure changes and the interlayer coupling effects in bilayer black phosphorus underscores the material's unique response to the strain and highlights the need for a more profound understanding of its thermal properties. Subsequently, we will present a comprehensive explanation of how the modification of interlayer coupling enhances phonon transport.

We are aware of prior studies highlighting the substantial influence of the interlayer strain variations on the phonon hydrodynamic transport [54]. Phonon hydrodynamics, characterized by the collective phonon flow and viscous interactions, has the potential to enhance the phonon transport more effectively than conventional Fourier heat conduction. Notably, phonon hydrodynamics occurs when N-process scattering (encompassing normal phonon-phonon scattering mechanisms) predominates over U-process scattering (associated with umklapp processes). Therefore, in the following, our investigation aims to elucidate the intricate interplay between the strain-induced modifications, the interlayer interactions, and their effects on phonon hydrodynamics to comprehend the non-monotonic behavior in thermal conductivity induced by strain. Before exploring their effects on phonon hydrodynamics, we first demonstrate the occurrence of phonon hydrodynamics in bilayer black phosphorus by calculating separated N-process and U-process scattering for a comparison with representative materials, including monolayer graphene, AB-stacked bilayer graphene, and graphene+ [71–73] (details shown in Supplemental Material Sec. III [65]).

Notably, the primary factor contributing to robust phonon hydrodynamic transport in 2D materials is the prevalence of N-type scattering and the large density of states of long-wavelength Z-axis acoustic (ZA) phonons [40]. This characteristic is attributed to the quadratic dispersion predicted by continuum elasticity theory, considered as a universal feature of 2D materials [74,75]. Additionally, previous research has shed light on the fascinating interplay between charges and atoms in bilayer materials, particularly in the context of quasicovalent bonds. These quasibonds form as a result of charge redistribution and interaction, which play a pivotal role in the behavior of materials like bilayer black phosphorus. In Fig. 4(a), we present a charge difference density profile that reveals how the coupling strength of the interlayer lone electron pairs is intensified with the increasing strain. This enhancement of quasicovalent bonding signifies a more pronounced sharing of electrons between adjacent layers in bilayer black phosphorous. The fundamental physical mechanism at play involves a shift in strain, impacting interlayer coupling and consequently softening all optical modes, as illustrated in Fig. 2(a) [76]. This softening signifies a reduction in intralayer bonding strength between atoms, arising from the transfer of lone electron pairs from intralayer P-P covalent bonds to interlayer quasicovalent bonds, effectively fortifying these quasicovalent bonds [23].

These reinforced quasicovalent bonds play a crucial role in maintaining and even strengthening the quadratic morphology of the ZA mode in bilayer black phosphorus, as illustrated in Fig. 4(b). This stands in stark contrast to the strain-induced linearization of the quadratic ZA mode observed in AB-stacked bilayer graphene and single-layer black phosphorus (see details in Supplemental Material Fig. S6 [65]). The rationale is straightforward: introducing strain to AB-stacked bilayer graphene and monolayer black phosphorus disrupts the rigid rotational invariance of the forces acting on each particle, ultimately resulting in the linearization of the ZA mode [77,78]. Conversely, in bilayer black phosphorus, the enhanced interaction of quasicovalent bonds impedes structural deformation, thereby preserving and even strengthening the quadratic behavior of the ZA mode. Therefore, the intricate competition among strain-induced softening of optical phonons, subsequent enhancement of phonon scattering, and the maintenance/strengthening of the quadratic ZA mode through strengthened quasibonds, benefitting phonon hydrodynamics, is the key factor underlying the observed nonmonotonic behavior in phonon hydrodynamic transport. As a result, as depicted in Fig. 4(c), the phonon scattering rate demonstrates a clearer observation of the nonmonotonic dependence of the phonon scattering rate on strain. Specifically, at a strain of 2%, the scattering rate at low frequency is notably smaller compared to strains of 1% and 3%. Additionally, we
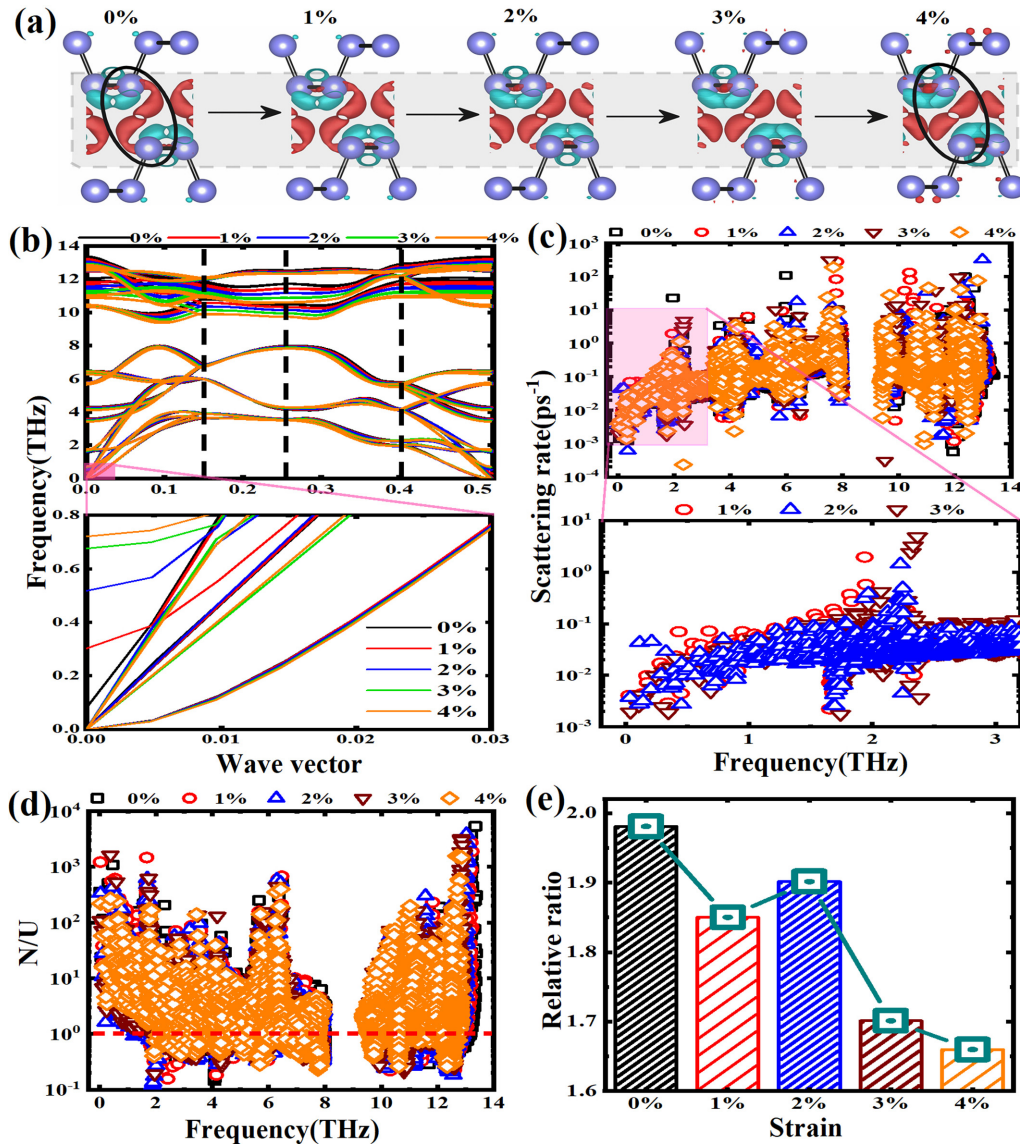
FIG. 4. Charge density difference profile, phonon dispersion, and the frequency-resolved scattering rates. (a) The evolution of the charge density difference in bilayer black phosphorus with increasing strain. The green and red regions indicate electron loss and gain, respectively. (b) The phonon dispersion, (c) the scattering rates, (d) the normal to umklapp (*N/U*) scattering process ratio, and (e) the ensemble-averaged *N/U* scattering process ratio in black phosphorus within a smaller strain range.

analyzed Grüneisen parameters across varying strains, with a specific focus on the low-frequency spectrum ranging 1–3% strain. Deviations of the Grüneisen parameter from zero provide insight into the level of anharmonicity within the system. Results indicate that under 2% strain, the Grüneisen parameter displays a more concentrated distribution around zero compared to 1% and 3%, indicating reduced anharmonicity and consequently weaker phonon scattering rates (see Supplemental Material Sec. IV for details [65]).

However, it is crucial to acknowledge that the current scattering rate calculations in Fig. 4(c) do not provide a comprehensive explanation of how the interlayer coupling modulates the phonon hydrodynamic phenomena, as they do not differentiate between *N*-type and *U*-type scattering. There has been a significant amount of research work that identifies whether phonon hydrodynamic transport occurs in materials by distinguishing between *N/U* scattering [29,35,48,49]. To

bridge this research gap, we employ the definitions of the *N*-type and *U*-type scattering for phonons, enabling us to distinguish between these two scattering mechanisms. The results of this comprehensive analysis are presented in Fig. 4(d), illustrating the ratio of *N*-type scattering to *U*-type scattering. Importantly, it is evident from these results that in a substantial portion of the spectrum, the values exceed 1, indicating the prevalent occurrence of *N*-type scattering. This compelling observation strongly suggests the presence of phonon hydrodynamic phenomena within the structure of bilayer black phosphorus. Furthermore, to facilitate a more accessible comparison of the dominance between the *N*-type and *U*-type scattering, we calculate the ensemble-averaged scattering rate employing the equation [41]

$$\bar{\Gamma}_i = \frac{\sum C_\lambda \Gamma_{\lambda,i}}{\sum C_\lambda}, \qquad (2)$$

where i denotes N- or U-type scattering, and $C_\lambda = \frac{1}{k_B T^2} \sum_\lambda f_0 (f_0 + 1)(\hbar\omega_\lambda)^2$ is the specific heat of the phonon mode λ. This calculation, as depicted in Fig. 4(e), reveals a nonmonotonic behavior in the ratio of the N/U scattering process at different strain levels. This pattern initially exhibits a decrease, followed by an increase, and ultimately another decrease. Importantly, this nonmonotonic phenomenon in phonon scattering behavior aligns with the observed changes in the thermal conductivity of bilayer black phosphorus. This juncture marks a pivotal turning point where the underlying reasons for the nonmonotonic behavior in thermal conductivity begin to emerge. It underscores the crucial role played by strain in the modulation of bilayer black phosphorus, primarily through the alteration of the relative strength of the phonon hydrodynamics.

Up to this point, we have presented a different perspective on the modulation of phonon hydrodynamics within bilayer black phosphorus. Through the differentiation of the N-type and U-type scattering, we have unveiled a nonmonotonic trend in phonon scattering, closely mirroring the observed changes in thermal conductivity under strain in bilayer black phosphorus. This revolutionary insight significantly advances our understanding of how structural alterations impact the thermal performance of this material, ushering in different avenues for precisely controlling thermal conductivity in the two-dimensional materials.

This study offers significant insight into the intricate relationship between the strain and the modulation of phonon hydrodynamics in bilayer black phosphorus. Nonetheless, it is essential to acknowledge a significant limitation. Our investigation primarily accounts for third-order phonon interactions, overlooking the potential significance of the higher-order interaction terms. These higher-order effects, including nonlinear interactions and temperature influences, may exert a substantial influence on phonon hydrodynamics [36,46]. Addressing this limitation by incorporating higher-order phonon interactions is crucial for advancing our understanding of phonon hydrodynamics. Future research endeavors in this direction can unlock the full potential of this phenomenon, leading to transformative applications in nanotechnology and thermal management.

Despite the limitation, our study holds promise and opens up exciting perspectives in the field of phonon hydrodynamics. The current research serves as a pioneering exploration into the modulation of phonon hydrodynamics, offering valuable insight into the complex interplay between strain and thermal conductivity in bilayer black phosphorus. By introducing the concept of distinguishing between N-type and U-type scattering, this study not only enhances our understanding of the fundamental phonon transport mechanisms but also lays the foundation for innovative strategies to control thermal behavior in two-dimensional materials. The ability to tailor phonon hydrodynamics has profound implications for various applications, from advanced thermal management in nanodevices to the design of materials with enhanced thermal performance.

IV. SUMMARY

This study investigates the intricate thermal behavior of bilayer black phosphorus under strain, providing deeper insight into phonon hydrodynamics within 2D materials. Employing advanced computational methods, we discover that, as strain increases, thermal conductivity typically decreases, but a nonmonotonic pattern emerges at lower strains, challenging conventional expectations. This intriguing behavior is attributed to a complex interplay between the structural changes and the interlayer quasicovalent bonds. Moreover, our findings underscore the dominant role of interlayer thickness in modulating these effects. In summary, our study demonstrates control of phonon hydrodynamics, providing valuable insight into thermal properties of 2D materials, especially for nanoscale thermal management. Crucially, our findings highlight the potential of harnessing in-plane strain to modulate phonon hydrodynamics and thermal transport in non-vdW-dominated 2D materials. This discovery unlocks fresh possibilities for the design and optimization of nanoscale thermal management and energy conversion devices.

ACKNOWLEDGMENTS

[1] Y. Ouyang, Z. Zhang, D. Li, J. Chen, and G. Zhang, Emerging theory, materials, and screening methods: New opportunities for promoting thermoelectric performance, Ann. Phys. **531**, 1800437 (2019).

[2] J. Chen, X. Xu, J. Zhou, and B. Li, Interfacial thermal resistance: Past, present, and future, Rev. Mod. Phys. **94**, 025002 (2022).

[3] X. Qian, J. Zhou, and G. Chen, Phonon-engineered extreme thermal conductivity materials, Nat. Mater. **20**, 1188 (2021).

[4] S. Hu, Z. Zhang, P. Jiang, W. Ren, C. Yu, J. Shiomi, and J. Chen, Disorder limits the coherent phonon transport in two-dimensional phononic crystal structures, Nanoscale **11**, 11839 (2019).

[5] Y. Liu, W. Ren, M. An, L. Dong, L. Gao, X. Shai, T. Wei, L. Nie, S. Hu, and C. Zeng, A qualitative study of the disorder effect on the phonon transport in a two-dimensional graphene/h-BN heterostructure, Front. Mater. **9**, 913764 (2022).

[6] Z. Zhang, Y. Guo, M. Bescond, M. Nomura, S. Volz, and J. Chen, Assessing phonon coherence using spectroscopy, Phys. Rev. B **107**, 155426 (2023).

[7] Y. Guo, Z. Zhang, M. Bescond, S. Xiong, M. Nomura, and S. Volz, Anharmonic phonon-phonon scattering at the interface between two solids by nonequilibrium green's function formalism, Phys. Rev. B **103**, 174306 (2021).

[8] M. Nomura, R. Anufriev, Z. Zhang, J. Maire, Y. Guo, R. Yanagisawa, and S. Volz, Review of thermal

transport in phononic crystals, Mater. Today Phys. **22**, 100613 (2022).

[9] X. Huang, Y. Guo, Y. Wu, S. Masubuchi, K. Watanabe, T. Taniguchi, Z. Zhang, S. Volz, T. Machida, and M. Nomura, Observation of phonon poiseuille flow in isotopically purified graphite ribbons, Nat. Commun. **14**, 2044 (2023).

[10] D. Çakır, H. Sahin, and F. M. Peeters, Tuning of the electronic and optical properties of single-layer black phosphorus by strain, Phys. Rev. B **90**, 205421 (2014).

[11] A. S. Rodin, A. Carvalho, and A. H. Castro Neto, Strain-induced gap modification in black phosphorus, Phys. Rev. Lett. **112**, 176801 (2014).

[12] J. Guan, W. Song, L. Yang, and D. Tománek, Strain-controlled fundamental gap and structure of bulk black phosphorus, Phys. Rev. B **94**, 045414 (2016).

[13] H. Liu, J.-T. Sun, C. Cheng, F. Liu, and S. Meng, Photoinduced nonequilibrium topological states in strained black phosphorus, Phys. Rev. Lett. **120**, 237403 (2018).

[14] M. Alidoust, K. Halterman, D. Pan, M. Willatzen, and J. Akola, Strain-engineered widely tunable perfect absorption angle in black phosphorus from first principles, Phys. Rev. B **102**, 115307 (2020).

[15] S. Huang, Y. Lu, F. Wang, Y. Lei, C. Song, J. Zhang, Q. Xing, C. Wang, Y. Xie, L. Mu, G. Zhang, H. Yan, B. Chen, and H. Yan, Layer-dependent pressure effect on the electronic structure of 2D black phosphorus, Phys. Rev. Lett. **127**, 186401 (2021).

[16] T. Loippo, A. Kanniainen, and J. T. Muhonen, Strain effects in phosphorus bound exciton transitions in silicon, Phys. Rev. Mater. **7**, 016202 (2023).

[17] G. Qin, X. Zhang, S.-Y. Yue, Z. Qin, H. Wang, Y. Han, and M. Hu, Resonant bonding driven giant phonon anharmonicity and low thermal conductivity of phosphorene, Phys. Rev. B **94**, 165445 (2016).

[18] J.-W. Jiang and H. S. Park, Negative poisson's ratio in single-layer black phosphorus, Nat. Commun. **5**, 4727 (2014).

[19] J.-W. Jiang, Thermal conduction in single-layer black phosphorus: Highly anisotropic? Nanotechnology **26**, 055701 (2015).

[20] L. Han, Y. Zou, Q. Zeng, X. Guan, B. Jia, Y. Gao, G. Liu, and L. Wu, Strong interlayer interaction in two-dimensional layered PtTe2, J. Solid State Chem. **305**, 122657 (2022).

[21] N. Mao, Y. Lin, Y.-Q. Bie, T. Palacios, L. Liang, R. Saito, X. Ling, J. Kong, and W. A. Tisdale, Resonance-enhanced excitation of interlayer vibrations in atomically thin black phosphorus, Nano Lett. **21**, 4809 (2021).

[22] X. Luo, X. Lu, G. K. W. Koon, A. H. Castro Neto, B. Özyilmaz, Q. Xiong, and S. Y. Quek, Large frequency change with thickness in interlayer breathing mode—significant interlayer interactions in few layer black phosphorus, Nano Lett. **15**, 3931 (2015).

[23] Z.-X. Hu, X. Kong, J. Qiao, B. Normand, and W. Ji, Interlayer electronic hybridization leads to exceptional thickness-dependent vibrational properties in few-layer black phosphorus, Nanoscale **8**, 2740 (2016).

[24] J. Qiao, X. Kong, Z.-X. Hu, F. Yang, and W. Ji, High-mobility transport anisotropy and linear dichroism in few-layer black phosphorus, Nat. Commun. **5**, 4475 (2014).

[25] S. Dong *et al.*, Ultralow-frequency collective compression mode and strong interlayer coupling in multilayer black phosphorus, Phys. Rev. Lett. **116**, 087401 (2016).

[26] X. Peng, Q. Wei, and A. Copple, Strain-engineered direct-indirect band gap transition and its mechanism in two-dimensional phosphorene, Phys. Rev. B **90**, 085402 (2014).

[27] M. Elahi, K. Khaliji, S. M. Tabatabaei, M. Pourfath, and R. Asgari, Modulation of electronic and mechanical properties of phosphorene through strain, Phys. Rev. B **91**, 115412 (2015).

[28] E. Taghizadeh Sisakht, F. Fazileh, M. H. Zare, M. Zarenia, and F. M. Peeters, Strain-induced topological phase transition in phosphorene and in phosphorene nanoribbons, Phys. Rev. B **94**, 085417 (2016).

[29] C. Yu, S. Shan, S. Lu, Z. Zhang, and J. Chen, Characteristics of distinct thermal transport behaviors in single-layer and multilayer graphene, Phys. Rev. B **107**, 165424 (2023).

[30] R. A. Guyer and J. A. Krumhansl, Thermal conductivity, second sound, and phonon hydrodynamic phenomena in nonmetallic crystals, Phys. Rev. **148**, 778 (1966).

[31] L. Sendra, A. Beardo, P. Torres, J. Bafaluy, F. X. Alvarez, and J. Camacho, Derivation of a hydrodynamic heat equation from the phonon boltzmann equation for general semiconductors, Phys. Rev. B **103**, L140301 (2021).

[32] P. Scuracchio, K. H. Michel, and F. M. Peeters, Phonon hydrodynamics, thermal conductivity, and second sound in two-dimensional crystals, Phys. Rev. B **99**, 144303 (2019).

[33] Y. Guo, Z. Zhang, M. Bescond, S. Xiong, M. Wang, M. Nomura, and S. Volz, Size effect on phonon hydrodynamics in graphite microstructures and nanostructures, Phys. Rev. B **104**, 075450 (2021).

[34] Y. Guo and M. Wang, Phonon hydrodynamics for nanoscale heat transport at ordinary temperatures, Phys. Rev. B **97**, 035421 (2018).

[35] Z. Zhang, Y. Ouyang, Y. Guo, T. Nakayama, M. Nomura, S. Volz, and J. Chen, Hydrodynamic phonon transport in bulk crystalline polymers, Phys. Rev. B **102**, 195302 (2020).

[36] M.-Y. Shang, W.-H. Mao, N. Yang, B. Li, and J.-T. Lü, Unified theory of second sound in two-dimensional materials, Phys. Rev. B **105**, 165423 (2022).

[37] Y. Machida, A. Subedi, K. Akiba, A. Miyake, M. Tokunaga, Y. Akahama, K. Izawa, and K. Behnia, Observation of poiseuille flow of phonons in black phosphorus, Sci. Adv. **4**, eaat3374 (2018).

[38] V. Martelli, J. L. Jiménez, M. Continentino, E. Baggio-Saitovitch, and K. Behnia, Thermal transport and phonon hydrodynamics in strontium titanate, Phys. Rev. Lett. **120**, 125901 (2018).

[39] A. Beardo, M. G. Hennessy, L. Sendra, J. Camacho, T. G. Myers, J. Bafaluy, and F. X. Alvarez, Phonon hydrodynamics in frequency-domain thermoreflectance experiments, Phys. Rev. B **101**, 075303 (2020).

[40] S. Lee, D. Broido, K. Esfarjani, and G. Chen, Hydrodynamic phonon transport in suspended graphene, Nat. Commun. **6**, 6290 (2015).

[41] A. Cepellotti, G. Fugallo, L. Paulatto, M. Lazzeri, F. Mauri, and N. Marzari, Phonon hydrodynamics in two-dimensional materials, Nat. Commun. **6**, 6400 (2015).

[42] Y. Hu, D. Li, Y. Yin, S. Li, G. Ding, H. Zhou, and G. Zhang, The important role of strain on phonon hydrodynamics in diamond-like Bi-layer graphene, Nanotechnology **31**, 335711 (2020).

[43] S. Huberman, R. A. Duncan, K. Chen, B. Song, V. Chiloyan, Z. Ding, A. A. Maznev, G. Chen, and K. A. Nelson, Observation of

second sound in graphite at temperatures above 100 K, Science **364**, 375 (2019).

[44] P. Torres, F. X. Alvarez, X. Cartoixà, and R. Rurali, Thermal conductivity and phonon hydrodynamics in transition metal dichalcogenides from first-principles, 2D Mater. **6**, 035002 (2019).

[45] Y. Machida, N. Matsumoto, T. Isono, and K. Behnia, Phonon hydrodynamics and ultrahigh–room-temperature thermal conductivity in thin graphite, Science **367**, 309 (2020).

[46] Y. Guo and M. Wang, Phonon hydrodynamics and its applications in nanoscale heat transport, Phys. Rep. **595**, 1 (2015).

[47] S. Lee and X. Li, Hydrodynamic Phonon Transport: Past,Present and Prospects, in *Nanoscale Energy Transport*, edited by B. Liao (IOP, Bristol, 2020), pp. 1–26.

[48] Z. Ding, J. Zhou, B. Song, V. Chiloyan, M. Li, T.-H. Liu, and G. Chen, Phonon hydrodynamic heat conduction and knudsen minimum in graphite, Nano Lett. **18**, 638 (2018).

[49] X. Li, H. Lee, E. Ou, S. Lee, and L. Shi, Reexamination of hydrodynamic phonon transport in thin graphite, J. Appl. Phys. **131**, 075104 (2022).

[50] X. Li and S. Lee, Role of hydrodynamic viscosity on phonon transport in suspended graphene, Phys. Rev. B **97**, 094309 (2018).

[51] Z. Ding, K. Chen, B. Song, J. Shin, A. A. Maznev, K. A. Nelson, and G. Chen, Observation of second sound in graphite over 200 K, Nat. Commun. **13**, 285 (2022).

[52] J. Jeong, X. Li, S. Lee, L. Shi, and Y. Wang, Transient hydrodynamic lattice cooling by picosecond laser irradiation of graphite, Phys. Rev. Lett. **127**, 085901 (2021).

[53] A. Beardo, M. López-Suárez, L. A. Pérez, L. Sendra, M. I. Alonso, C. Melis, J. Bafaluy, J. Camacho, L. Colombo, R. Rurali, F. X. Alvarez, and J. S. Reparaz, Observation of second sound in a rapidly varying temperature field in Ge, Sci. Adv. **7**, eabg4677 (2021).

[54] F. Duan, C. Shen, H. Zhang, and G. Qin, Hydrodynamically enhanced thermal transport due to strong interlayer interactions: A case study of strained bilayer graphene, Phys. Rev. B **105**, 125406 (2022).

[55] A. Ward, D. A. Broido, D. A. Stewart, and G. Deinzer, Ab initio theory of the lattice thermal conductivity in diamond, Phys. Rev. B **80**, 125203 (2009).

[56] Y. Chen, J. Ma, and W. Li, Understanding the thermal conductivity and lorenz number in tungsten from first principles, Phys. Rev. B **99**, 020305(R) (2019).

[57] J. Ma, W. Li, and X. Luo, Examining the callaway model for lattice thermal conductivity, Phys. Rev. B **90**, 035203 (2014).

[58] L. Lindsay, D. A. Broido, and T. L. Reinecke, Ab initio thermal transport in compound semiconductors, Phys. Rev. B **87**, 165201 (2013).

[59] G. Kresse and J. Furthmüller, Efficient iterative schemes for ab initio total-energy calculations using a plane-wave basis set, Phys. Rev. B **54**, 11169 (1996).

[60] J. P. Perdew, K. Burke, and M. Ernzerhof, Generalized gradient approximation made simple, Phys. Rev. Lett. **77**, 3865 (1996).

[61] J. Klimeš, D. R. Bowler, and A. Michaelides, Van Der Waals density functionals applied to solids, Phys. Rev. B **83**, 195131 (2011).

[62] H. J. Monkhorst and J. D. Pack, Special points for brillouin-zone integrations, Phys. Rev. B **13**, 5188 (1976).

[63] A. Togo, F. Oba, and I. Tanaka, First-principles calculations of the ferroelastic transition between rutile-type and $CaCl_2$-Type SiO_2 at high pressures, Phys. Rev. B **78**, 134106 (2008).

[64] W. Li, J. Carrete, N. A. Katcho, and N. Mingo, ShengBTE: A solver of the boltzmann transport equation for phonons, Comput. Phys. Commun. **185**, 1747 (2014).

[65] See Supplemental Material at http://link.aps.org/supplemental/10.1103/PhysRevB.109.165413 for detailed information on close neighbor and Q-grid density testing, the influence of strain on phonon dispersion and scattering phase space in bilayer black phosphorus, a demonstration of phonon hydrodynamics, and the calculation of Grüneisen parameters under various strains. It also contains Refs. [35,54–58,71–73,79].

[66] S. Huang, G. Zhang, F. Fan, C. Song, F. Wang, Q. Xing, C. Wang, H. Wu, and H. Yan, Strain-tunable van Der Waals interactions in few-layer black phosphorus, Nat. Commun. **10**, 2447 (2019).

[67] R. Fei and L. Yang, Strain-engineering the anisotropic electrical conductance of few-layer black phosphorus, Nano Lett. **14**, 2884 (2014).

[68] D. Tristant, A. Cupo, X. Ling, and V. Meunier, Phonon anharmonicity in few-layer black phosphorus, ACS Nano **13**, 10456 (2019).

[69] B. Mortazavi, E. V. Podryabinkin, I. S. Novikov, T. Rabczuk, X. Zhuang, and A. V. Shapeev, Accelerating first-principles estimation of thermal conductivity by machine-learning interatomic potentials: A MTP/ShengBTE solution, Comput. Phys. Commun. **258**, 107583 (2021).

[70] A. Jain and A. J. H. McGaughey, Strongly anisotropic in-plane thermal transport in single-layer black phosphorene, Sci. Rep. **5**, 8501 (2015).

[71] Y. Guo, Phonon vortex dynamics in graphene ribbon by solving boltzmann transport equation with ab initio scattering rates, Int. J. Heat Mass Transfer **169**, 120981 (2021).

[72] L. Yu, A. Chen, X. Wang, H. Wang, Z. Qin, and G. Qin, Softened $sp2 - sp3$ bonding network leads to strong anharmonicity and weak hydrodynamics in graphene+, Phys. Rev. B **106**, 125410 (2022).

[73] J. Jiang, S. Lu, Y. Ouyang, and J. Chen, How hydrodynamic phonon transport determines the convergence of thermal conductivity in two-dimensional materials, Nanomaterials **12**, 2854 (2022).

[74] R. Roldán, A. Fasolino, K. V. Zakharchenko, and M. I. Katsnelson, Suppression of anharmonicities in crystalline membranes by external strain, Phys. Rev. B **83**, 174104 (2011).

[75] L. Landau and E. Lifshitz, *Theory of Elasticity* (Pergamon Press, Oxford, 1995).

[76] Y. Du, J. Maassen, W. Wu, Z. Luo, X. Xu, and P. D. Ye, Auxetic black phosphorus: A 2D material with negative poisson's ratio, Nano Lett. **16**, 6701 (2016).

[77] J. Carrete, W. Li, L. Lindsay, D. A. Broido, L. J. Gallego, and N. Mingo, Physically founded phonon dispersions of few-layer materials and the case of borophene, Mater. Res. Lett. **4**, 204 (2016).

[78] A. Taheri, S. Pisana, and C. V. Singh, Importance of quadratic dispersion in acoustic flexural phonons for thermal transport of two-dimensional materials, Phys. Rev. B **103**, 235426 (2021).

[79] Y. Zhang, X. Ke, C. Chen, J. Yang, and P. R. C. Kent, Thermodynamic properties of PbTe, PbSe, and PbS: First-principles study, Phys. Rev. B **80**, 024304 (2009).